Journal of Molecular Catalysis A: Chemical 328 (2010) 53–59

Contents lists available at ScienceDirect

Journal of Molecular Catalysis A: Chemical

journal homepage: www.elsevier.com/locate/molcata

Selective surface modification of activated carbon for enhancing the catalytic performance in hydrogen peroxide production by hydroxylamine oxidation

Wei Song, Yong Li, Xiaohui Guo, Juan Li, Xiumin Huang, Wenjie Shen*

State Key Laboratory of Catalysis, Dalian Institute of Chemical Physics, Chinese Academy of Sciences, Dalian 116023, China

ARTICLE INFO

Article history:
Received 4 November 2009
Received in revised form 28 March 2010
Accepted 31 May 2010
Available online 8 June 2010

Keywords:
Hydrogen peroxide
Activated carbon
Surface chemistry
Selective modification
$KMnO_4$ oxidation

ABSTRACT

The textural structure and the surface property of activated carbon were selectively modified by $KMnO_4$ oxidation. The activated carbon treated by $KMnO_4$ oxidation in an acidic solution showed greatly enhanced H_2O_2 production by hydroxylamine oxidation due to the creation of more surface quinoid species, and the yield of hydrogen peroxide approached 78% (0.66 wt.%). Structure and surface analyses revealed that $KMnO_4$ oxidation in the acidic solution produced more phenolic but less carboxylic groups on the activated carbon, confirming the crucial role of the quinoid groups. It was further proposed that the quinoid groups serving as electron acceptors and redox mediators involved in the formation of H_2O_2 through a redox cycle.

1. Introduction

Hydrogen peroxide (H_2O_2) is one of the most environmentally benign oxidants and it is widely used in fine chemical synthesis, paper bleaching and waste water treatment [1]. Nowadays, H_2O_2 is mainly produced through the anthraquinone auto-oxidation (AO) process, which is a multi-step, energy-consuming and waste generating process. The economics of this commercial process only depends on large-scale production with effective recycling of the organic solution and the hydrogenation catalyst. Moreover, this process produces concentrated H_2O_2, which is usually far from the requirement of relatively low concentration of H_2O_2 in most practical applications [2,3]. Therefore, in situ and small-scale production of H_2O_2 has attracted extensive attention. In this context, the synthesis of H_2O_2 from hydrogen and oxygen molecules over palladium catalysts has been developed [4,5]. However, this atom-efficient and green process is hindered by the risk of explosion related to the direct mixing of O_2 and H_2 and the non-selective formation of water [6].

Hydroxylamine (NH_2OH) is a strong reductive agent and can be easily oxidized by molecular oxygen or air into H_2O_2 at ambient conditions in water [7,8]. Hence, the direct production of H_2O_2 from NH_2OH and O_2 is regarded as a simple and clean process with nitrogen and water as the only by-products. To date, homogeneous manganese complexes [9,10] and supported noble metals (Au and Pd) [11–13] have been reported to be effective for this reaction. In the homogeneous process, the turnover frequency (TOF) of NH_2OH could be as high as $10^4\ h^{-1}$ owing to the tiny amount of highly active Mn^{2+} species. Nevertheless, it suffers from the separation and recycle of the catalytic components. In the heterogeneous system, the catalysts can be easily separated and reused, but the high cost of precious metals and the low concentration of H_2O_2 (0.01–0.15 wt.%) are the major obstacles for the practical application.

We have recently reported that activated carbon (AC) without any precious metals acted as effective catalyst in the direct production of H_2O_2 from NH_2OH and O_2 [14]. The yield of H_2O_2 could be as high as 46% (H_2O_2 concentration, 0.39 wt.%), in which the surface oxygen-containing species on the ACs, especially the quinoid groups, played essential roles. Therefore, it is expected that the catalytic performance would be further promoted by creating more surface oxygen-containing species. Liquid-phase oxidation of AC with mineral acids, such as nitric acid, sulphuric acid or their mixture, is conventionally used to introduce surface oxygen functional groups. However, various types of surface oxygen-containing species like carboxyls, anhydrides, hydroxyls, lactones and quinoid groups are produced simultaneously [15]. Recently, selective treatment of carbon surface has been attracted much attention. Zhang et al. [16] have reported that oxidation with $KMnO_4$ in alkali solution is capable of creating more quinoid groups on the surface of carbon nanotubes. Additionally, $KMnO_4$ oxidation in acidic solution was found to yield less carboxylic groups but more surface defects on carbon nanofibers [17]. By considering the fact that the direct production of H_2O_2 from NH_2OH and O_2 requires more surface

* Corresponding author. Tel.: +86 411 84379085; fax: +86 411 84694447.
E-mail address: shen98@dicp.ac.cn (W. Shen).

1381-1169/$ – see front matter © 2010 Elsevier B.V. All rights reserved.
doi:10.1016/j.molcata.2010.05.022

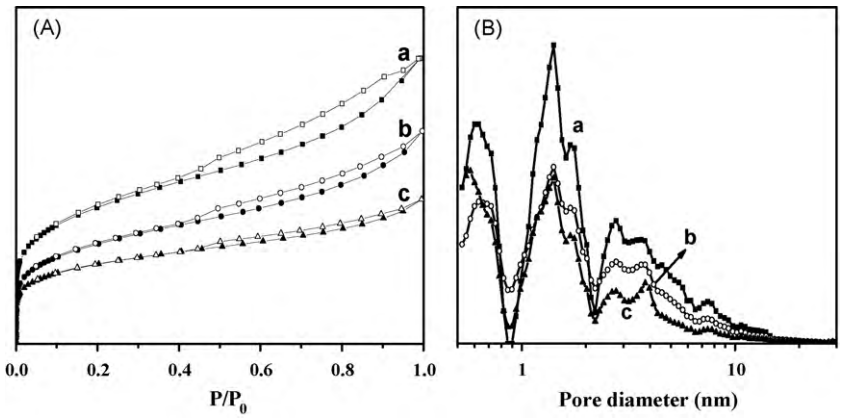

Fig. 1. N_2 adsorption–desorption isotherms (A) and pore size distributions (B) of the AC (a), ACA (b) and ACB (c) samples.

quinoid groups, in this work, we treat a commercial AC with aqueous $KMnO_4$ solutions under mild conditions in order to selectively modify the surface property. Correlation between the catalytic performance and the surface chemistry has been established and the possible reaction pathway has also been proposed.

2. Experiments

2.1. Surface modification

Five grams of activated carbon (200–300 mesh, Aldrich) was initially treated with 50 ml of concentrated hydrochloric acid (37%) to remove the inorganic impurities and ashes. The mixture was stirred at room temperature for 3 h, followed by thoroughly washing with hot water until the filtrate was free of Cl^- (detected by $AgNO_3$). The sample was dried at 110 °C overnight in vacuum, which was nominated as AC. Thereafter, 1.5 g of AC was mixed with 30 ml of 0.2 M $KMnO_4$ in 0.5 M H_2SO_4 or 0.2 M NaOH solutions. When treated in the acidic solution, the mixture was stirred at 70 °C for 6 h, and then filtered and washed with concentrated HCl (37%) to remove the MnO_2. When oxidized in the basic solution, the carbon slurry was refluxed for 40 min, and then 1.5 g of Na_2SO_3 was added, followed by the addition of 15 ml of 1 M H_2SO_4. Subsequently, both the samples were washed alternatively with water, 0.01 M NaOH, water, and 0.5 M HCl until the filtrate was neutral. The AC samples were dried at 110 °C overnight in vacuum, and denoted as ACA and ACB, respectively. Here, A and B refer to the AC sample oxidized by $KMnO_4$ in acidic and basic solutions, respectively.

2.2. Characterization of the AC samples

Nitrogen adsorption–desorption isotherms were recorded on a Micrometrics ASAP 2000 instrument at −196 °C. Before the measurement, the AC sample was outgassed at 150 °C overnight. The specific surface area (S_{BET}) was calculated by a multipoint Braunauer–Emmett–Teller (BET) analysis.

Chemical titration for quantitative analysis of the surface acidic groups was based on the Boehm method [18]. Four series of AC sample (0.5 g) were first added to four flasks (150 ml). Then, 50 ml of 0.05 M sodium hydrogen carbonate ($NaHCO_3$), sodium carbonate (Na_2CO_3), sodium hydroxide (NaOH) and sodium ethoxide ($NaOC_2H_5$) were added to the flasks, respectively. The flasks were then sealed and stirred at room temperature for 24 h. After recovering the solution by filtration, 10 ml of aliquots were titrated with 0.05 M of HCl and the surface oxygenated groups were determined according to the following assumptions: $NaHCO_3$ merely neutralizes carboxyls; lactones are decided by the difference between the groups neutralized by Na_2CO_3 and $NaHCO_3$; phenols are estimated by the difference between the groups neutralized by NaOH and Na_2CO_3; and carbonyls/quinones are determined by the difference between the groups neutralized by $NaOC_2H_5$ and NaOH [19].

The pH values of the suspension were measured by dispersing 0.4 g of carbon powder into 20 ml of water, and the suspensions were stirred overnight to reach equilibrium.

Fourier transformation infrared (FTIR) spectra of the AC samples were recorded with a Bruker Vector 22 spectrometer using KBr pallet containing 0.5 wt.% of AC.

X-ray photoelectron spectroscopy (XPS) measurements were performed with an ESCALAB MK-II spectrometer (VG Scientific Ltd., UK) using Al Kα radiation with an accelerated voltage of 20 kV. Charge effect was corrected by adjusting the binding energy (BE) of C 1s to 285.0 eV. The surface atomic ratio of O/C was calculated from the peak areas and the sensitivity factors of the elements [20].

Temperature-programmed desorption (TPD) was conducted with a U-type quartz tubular reactor connected to a quadrupole mass spectrometer (Omnistar, Balzers). 40 mg of AC sample was loaded and heated to 900 °C at a rate of 10 °C/min under helium flow (30 ml/min) and the outlet gas was monitored by the mass spectrometer.

2.3. H_2O_2 production

The reaction of O_2 and NH_2OH was conducted in a jacketed glass reactor (100 ml) under stirring at ambient conditions (25 °C and atmospheric pressure), as described elsewhere [14]. Typically, the reaction mixture contained 0.15 g of AC catalyst and 1.74 g (25 mmol) of hydroxylammonium chloride ($NH_2OH{\cdot}HCl$) in 50 ml water. Before the addition of AC, the pH value of the aqueous solution was regulated to 8.6 by adding proper amounts of 1 M NaOH solution. O_2 (25 ml/min) was introduced through a mass flow controller into the reaction medium. Aliquots of the reaction mixture were withdrawn periodically and the concentration of H_2O_2 was analyzed using the colorimetric method based on titanium (IV) sulphate [21]. The yield of H_2O_2 was calculated according to the reaction stoichiometry ($2NH_2OH + O_2 = N_2 + 2H_2O + H_2O_2$). The concentration of $NH_2OH{\cdot}HCl$ was estimated by the colorimetric method according to the ferric complexes of Fe (III)-1,10-phenanthroline [22].

3. Results and discussion

3.1. Textural properties

Fig. 1 shows the N_2 adsorption–desorption isotherms of the AC samples. All the samples exhibited a combined characteristics of type I and type IV isotherms, indicating the presence of both

Table 1
Textural properties of the AC samples.

Sample	S_{BET} (m^2/g)[a]	S_{mic} (m^2/g)[b]	S_{mes} (m^2/g)[b]	V_{mic} (cm^3/g)[b]	V_{total} (cm^3/g)[c]
AC	1776	908	868	0.401	1.580
ACA	1293	647	646	0.288	1.178
ACB	1038	647	391	0.285	0.799

[a] Calculated using the BET theory.
[b] Estimated according to the *t*-plot method.
[c] Calculated from the amount of gas adsorbed at relative pressure of 0.992.

Table 2
Results of Boehm titration and pH measurements of the AC samples.

Sample	pH	Content of surface groups (mmol/g)				
		Carboxylic	Lactonic	Phenolic	Carbonylic	Total acidic
AC	4.70	0.244	0.194	0.137	0.129	0.704
ACA	3.19	1.097	0.558	1.147	0.366	3.167
ACB	2.51	1.421	0.542	0.557	0.633	3.153

micropores and mesopores. The relative small hysteresis loop of the ACB sample suggested the loss of large amounts of external surface during $KMnO_4$ oxidation in the basic solution. This is further confirmed by the pore size distributions of the AC samples. All the samples contained mesopores (50 nm > D_w > 2 nm), micropores (2 nm > D_w > 0.7 nm) and ultramicropores (D_w < 0.7 nm) [23], but the micropores and the mesopores decreased significantly after $KMnO_4$ treatments. Compared with the ACA sample, more mesopores were diminished in the ACB sample, indicating that severe surface erosion in the basic solution occurred.

Table 1 lists the textural parameters of the AC samples. After $KMnO_4$ oxidations, the pore structures were modified considerably. The specific surface area of the parent AC was 1776 m^2/g, but it decreased to 1293 m^2/g for the ACA sample and 1038 m^2/g for the ACB sample. Simultaneously, the mesoporous surface area decreased to 646 and 391 m^2/g for the ACA and ACB samples, respectively. On the other hand, the microporous surface area of the ACA and ACB samples was almost the same. It seems that $KMnO_4$ oxidation destroyed the pore structures to some extent, especially in the basic solution.

3.2. Surface chemistry

3.2.1. Boehm titration

Table 2 summarizes the results of Boehm titration and pH measurements of the AC samples. Apparently, the amounts of surface acidic groups increased greatly after $KMnO_4$ oxidations. The amounts of carboxylic groups increased significantly to 1.097 and 1.421 mmol/g for the ACA and ACB samples, respectively. Meanwhile, the amounts of phenolic groups enlarged greatly to 1.147 and 0.557 mmol/g for the ACA and ACB samples, respectively. Notably, more phenolic groups were generated on the surface of the ACA sample, which was almost two times larger than that of the ACB sample. Similar amount of lactones was formed on the ACA and ACB samples, and they were almost three times larger than that of the parent AC.

Generally, the pH value of the carbon suspension is related to the overall surface acidity. The ACA and ACB samples presented lower pH values than the parent AC, indicating the creation of more surface acidic groups. The pH value of the ACA sample (3.19) was higher than that of the ACB sample (2.51) although their total amounts of surface oxygen-containing groups were similar as determined by Boehm method. This implies that more carboxylic groups were generated on the surface of ACB sample by $KMnO_4$ oxidation in the basic solution, leading to a lower pH value. On the other hand, a significant increase in the quantity of phenolic groups was observed in the ACA sample due to the mild oxidation with $KMnO_4$ in the acidic solution. As a result, fewer amounts of carboxylic groups but more phenolic groups were generated in the ACA sample, resulting in a relative higher pH value.

3.2.2. FTIR

Fig. 2 shows the FTIR spectra of the AC samples. The band at 1240 cm^{-1} is assigned to C–O stretching and O–H bending molds in ethers, lactones, phenols and carboxylic anhydrides [20]. The band at 1580 cm^{-1} is associated with C=C double bond in quinone-like structure, while the band at 1720 cm^{-1} is due to C=O stretching vibration from lactones and carboxyl groups in the aromatic rings [24,25]. The intensities of these typical bands in the ACA and ACB samples were enhanced considerably. The bands at 1720 and 1240 cm^{-1} were relatively weak in the parent AC, indicating the less existence of carboxyls and phenols. These two bands in the ACA sample were enhanced greatly, suggesting that large amounts of carboxyls, lactones and phenols were generated. The band at 1720 cm^{-1} was the most intensive in the ACB sample, confirming

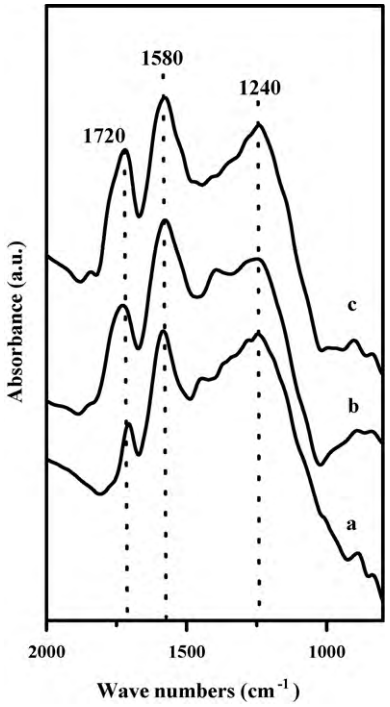

Fig. 2. FTIR spectra of the AC (a), ACA (b) and ACB (c) samples.

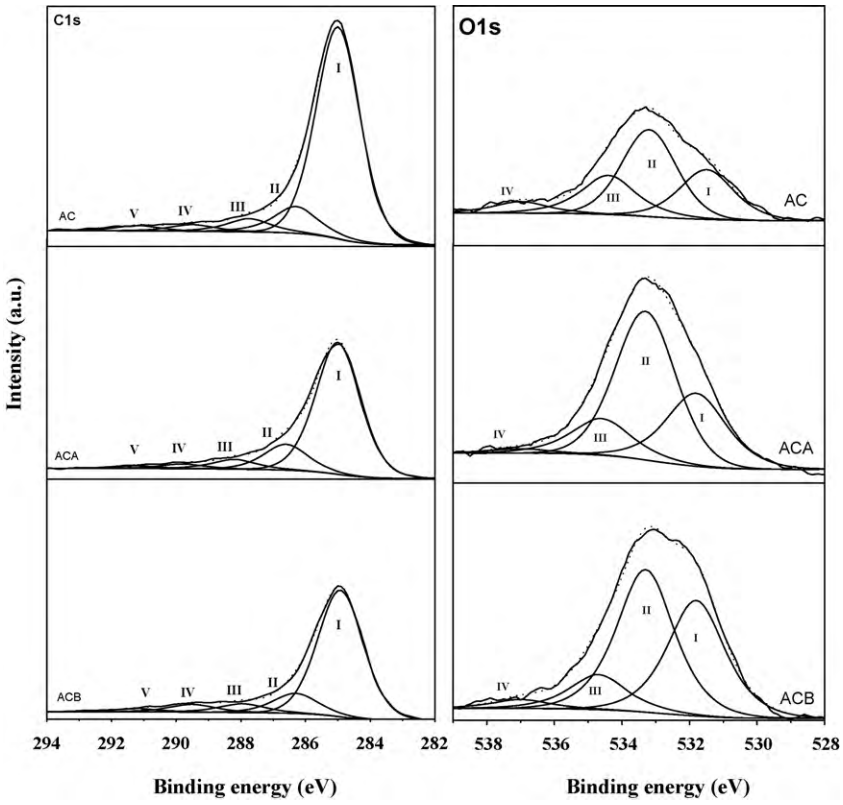

Fig. 3. The XPS spectra of C 1s and O 1s in the AC samples.

that the carboxylic groups were further enriched by $KMnO_4$ oxidation in the basic condition. This result is in good agreement with those of the Boehm titrations and pH measurements.

3.2.3. XPS

Fig. 3 shows the XPS spectra of C 1s spectra in the AC samples, and the detailed results of curve fitting are listed in Table 3. The C 1s spectra consisted of graphitic carbon (Peak I), phenolic, alcohol or ether groups (Peak II), carbonyl or quinone groups (Peak III), carboxyl acidic groups (Peak IV) and π–π^* shake-up satellite peak (Peak V) [26–28]. The oxidation of $KMnO_4$ decreased the intensities of Peak I and Peak V, but increased the intensities of the peaks ascribed to carbon–oxygen groups [27]. Notably, the area of Peak IV on the ACB sample (5.1%) was nearly two times larger than that of the ACA sample (2.8%), indicating that more carboxylic groups were produced by $KMnO_4$ oxidation in the basic solution, as confirmed by Boehm titration and IR measurement.

Fig. 3 also shows the XPS spectra of O 1s in the AC samples, and Table 4 summarizes the deconvolution results. Three main peaks corresponding to C=O (Peak I), C–O (Peak II) and adsorbed water or oxygen molecules (Peak III) were observed [26–28]. The minor Peak IV, with a binding energy at 537.0 eV, can be ascribed to adsorbed CO or CO_2 on the AC surface. Apparently, the intensities of Peak III and Peak IV lowered after $KMnO_4$ oxidation, but the peaks ascribed to carbon–oxygen groups intensified remarkably. The amount of C=O groups (Peak I) on the ACB sample was much large while the C–O groups (Peak II) on the ACA sample were relatively rich. This further confirms that more carboxylic groups were generated by $KMnO_4$ oxidation in the basic solution whereas more phenolic groups were produced by the mild oxidation in the acidic solution. Additionally, the surface O/C atomic ratios in the ACA and ACB samples enhanced greatly, indicating that surface oxygen-containing species can be effectively created by $KMnO_4$ oxidation.

3.2.4. TPD

Fig. 4 shows the TPD profiles of the AC samples. Upon heating, the surface oxygen-containing groups decompose into carbon oxides [20,29,30]. CO_2 desorption usually results from the decomposition of carboxylic acids/anhydrides at low temperatures or from the lactones at high temperatures; CO desorption originates from the carboxylic anhydrides, phenols, ethers, carbonyls and quinones [20]. Only small amounts of CO_x were detected on the parent AC but significant amounts of CO_x were detected on the ACA and ACB samples. Particularly, the amounts of CO desorbed from the ACA sample were nearly two times greater than that of the parent AC sample, confirming the creation of large amounts

Table 3
Deconvolution of the C 1s XPS profiles of the AC samples.

Sample	Functional groups/binding energy (eV)				
	Peak I C–graphite 284.9–285.0	Peak II C–O 286.3–286.5	Peak III C=O 287.8–288.1	Peak IV –COO– 289.5	Peak V π–π^* 291.2
AC	78.8	10.9	5.4	2.7	2.2
ACA	74.7	14.9	5.9	2.8	1.7
ACB	74.8	12.3	5.7	5.1	2.1

Table 4
Deconvolution of the O 1s XPS profiles of the AC samples.

Sample	Functional groups/binding energy (eV)				O/C (%)
	Peak I C=O 531.5–531.8	Peak II C–O 533.2–533.3	Peak III H_2O_{ads}, O_{2ads} 534.4–534.7	Peak IV CO_{2ads}, CO_{ads} 537.0	
AC	26.6	44.9	22.0	6.5	7.3
ACA	28.3	55.3	14.6	1.8	16.9
ACB	38.0	47.0	11.9	3.1	19.7

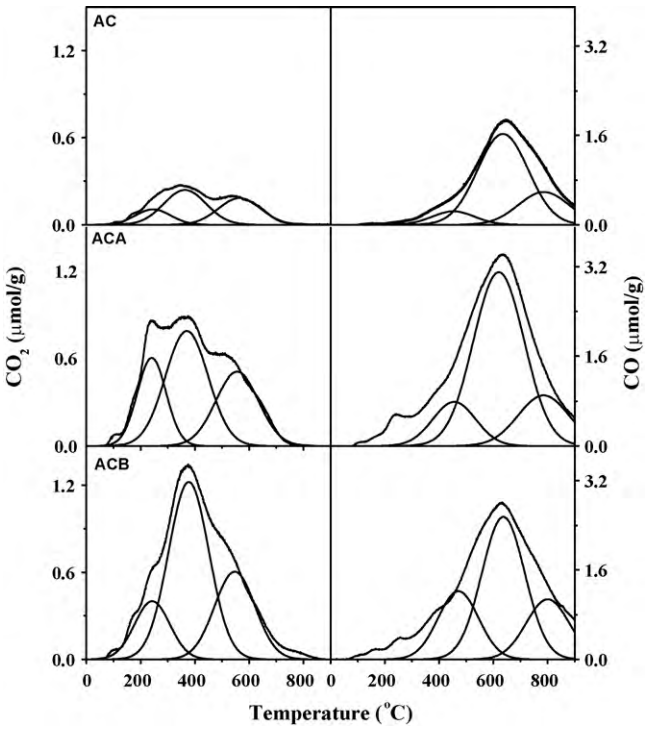

Fig. 4. TPD profiles of the AC, ACA and ACB samples.

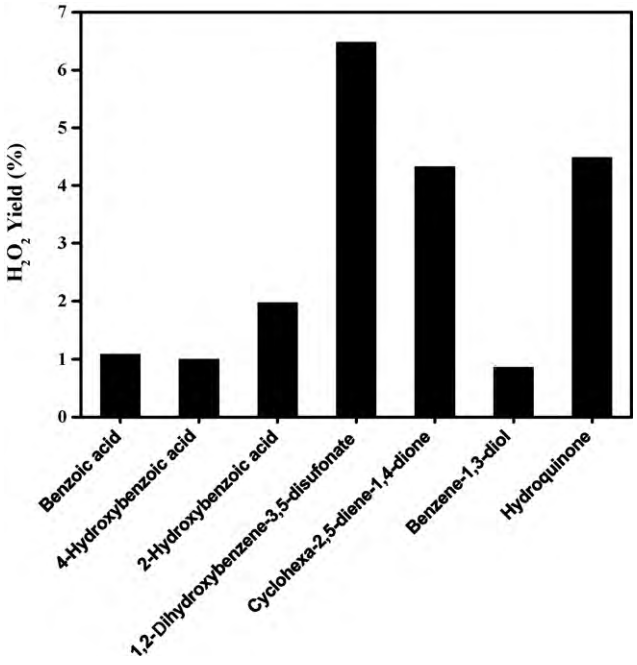

Fig. 6. H_2O_2 yields over the homogeneous catalysts.

of phenolic and carbonyl–quinone groups by $KMnO_4$ oxidation in the acidic solution. On the other hand, the amounts of CO_2 desorbed from the ACB sample were about five times larger than that of the parent AC mainly due to the significant formation of carboxylic acids/anhydrides by $KMnO_4$ oxidation in the basic solution.

Table 5 summarizes the amounts of specific surface groups. The amounts of CO_2 and CO desorbed from the parent AC were only 598 and 3386 μmol/g, respectively, but they remarkably increased to 2017 and 6561 μmol/g on the ACA sample. The amounts of CO_2 and CO desorbed from the ACB sample were 2436 and 5687 μmol/g, respectively. Compared with the ACA sample, more carboxylic

Table 5
Amounts of desorbed CO_2 and CO from the AC samples.

Sample	CO_2 (μmol/g)				CO (μmol/g)				Ratio[g]
	Carboxyl[a]	Anhydride[b]	Lacton[c]	Total	Anhydride[d]	Phenol[e]	Carbonyl–quinone[f]	Total	
AC	103	280	215	598	280	2283	823	3386	–
ACA	481	934	602	2017	934	4358	1269	6561	3.98
ACB	389	1370	677	2436	1370	3037	1280	5687	2.45

[a] Desorption temperature: 240–245 °C.
[b] Desorption temperature: 365–375 °C.
[c] Desorption temperature: 550–565 °C.
[d] Desorption temperature: 455–470 °C.
[e] Desorption temperature: 620–635 °C.
[f] Desorption temperature: 785–800 °C.
[g] The ratio of (phenolic and carbonyl–quinone)/(carboxylic and anhydride).

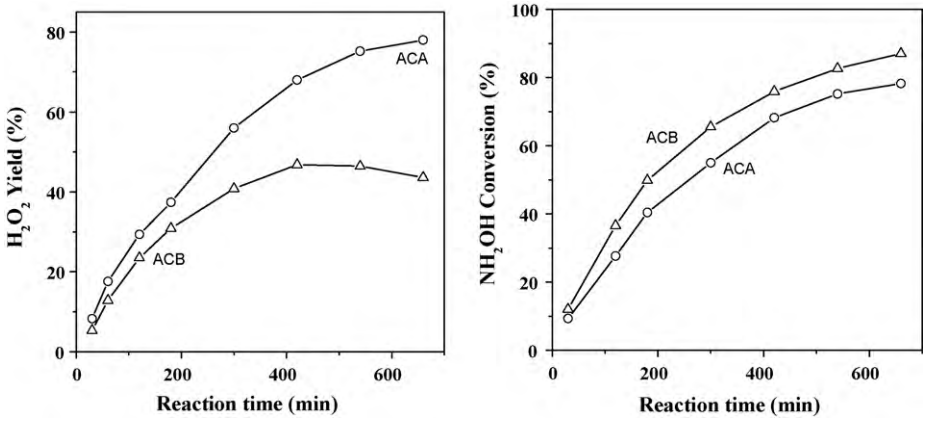

Fig. 5. H_2O_2 yields and NH_2OH conversions during NH_2OH oxidation over the AC catalysts.

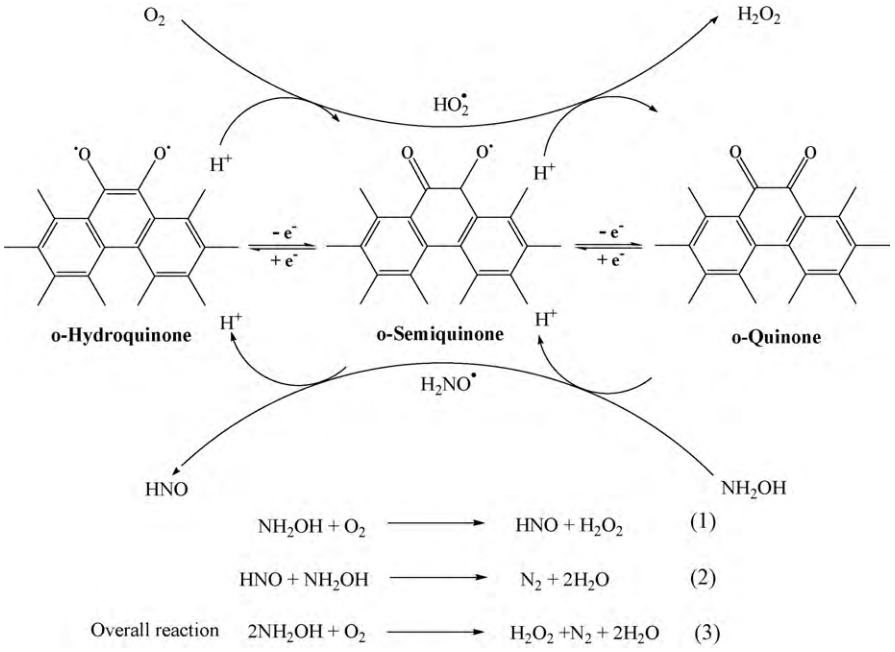

Fig. 7. A possible reaction pathway for NH_2OH oxidation over the AC catalyst.

groups but less phenolic groups were formed on the ACB sample. Almost the same amounts of lactones and carbonyl/quinones were obtained on both of the ACA and ACB samples. Therefore, $KMnO_4$ oxidation in the acidic solution favors to produce more phenolic groups rather than carboxylic groups in the basic solution.

3.3. H_2O_2 production

Fig. 5 shows the H_2O_2 yields and NH_2OH conversions during NH_2OH oxidation over the ACA and ACB catalysts. The yield of H_2O_2 remarkably increased during the initial stage and reached 30–40% after reaction for 200 min. On the ACB catalyst, the yield of H_2O_2 further increased to 47% at 420 min, followed by a slight decline. On the ACA catalyst, however, the yield of H_2O_2 significantly increased to 68% at 420 min and 78% at 660 min, showing a remarkably enhanced performance. At 60 min, the formation rates of H_2O_2 were 11.3×10^{-3} and 10.3×10^{-3} mmol/(m^2 h) over the ACA and ACB catalysts, respectively. When the reaction was performed for 660 min, however, the formation rate of H_2O_2 was 4.6×10^{-3} mmol/m^2 h over the ACA catalyst but it was only 3.2×10^{-3} mmol/m^2 h on the ACB catalyst, clearly demonstrating the higher activity of the ACA catalyst.

The ACA catalyst also exhibited a better selectivity towards H_2O_2 formation than the ACB catalyst. For example, the selectivity of H_2O_2 was as high as 92% over the ACA catalyst whereas it was only 62% over the ACB catalyst, although the conversion of NH_2OH was similar between the two samples. This is apparently related to the presence of more surface quinoid groups on the ACA catalyst, generated by the mild oxidation of $KMnO_4$ in the acidic solution. In the basic solution, however, the quinoid species might be further oxidized into carboxylic groups, which are not so effective for the production of H_2O_2. As shown in Table 5, the relative ratio of (phenolic and carbonyl–quinone)/(carboxylic and anhydride) over the ACA sample was 3.98, but it was only 2.45 on the ACB catalyst. Therefore, the higher catalytic performance of the ACA sample is straightforwardly attributed to the surface richness of quinoid species.

In order to identify the roles of the oxygen-containing species, homogeneous reactions were performed under the same reaction conditions using organic compounds containing carboxyl, phenol, quinone, or hydroquinone groups. As shown in Fig. 6, benzoic acid had a very low H_2O_2 yield, indicating that the carboxylic acids/anhydrides mainly enhanced the hydrophilicity to facilitate the contacts between the aqueous reactants and the active sites. 2-Hydroxybenzoic acid, 4-hydroxybenzoic acid and benzene-1,3-diol also showed low H_2O_2 yields, demonstrating that the phenol groups only possibly participated in the production of H_2O_2. In other words, the carboxylic acids/anhydrides and the phenols in the ACs are not the essential functional groups in the formation of H_2O_2. On the other hand, 1,2-dihydroxybenzene-3,5-disulfonate, disodium salt monohydrate (Tiron), cyclohexa-2,5-diene-1,4-dione, and hydroquinone gave much higher H_2O_2 yields, implying that the carbonyls and hydroxyls on the surfaces of the ACs might be the active species. Probably, the carbonyl pairs at the edge of the carbon layers behaving as quinones and the hydroxyl pairs acting as hydroquinones [31], are involved in the formation of H_2O_2 through a redox cycle.

Fig. 7 illustrates the possible reaction pathway of H_2O_2 formation. The quinone species (o-quinone) are initially reduced by NH_2OH to o-semiquinone and subsequently o-hydroquinone, NH_2OH loses protons and electrons, forming HNO. Then, o-hydroquinone is oxidized by molecular oxygen to o-quinone, releasing H_2O_2. The HNO intermediate reacts with NH_2OH, producing N_2 and H_2O. Here, NH_2OH is considered as a sacrificial reductant to convert o-quinone to the o-hydroquinone, similar to the reaction mechanism proposed in the homogeneous system [10]. In fact, this reaction route may start with any form of quinoid structures because the quinone–semiquinone–hydroquinone cycle could interact with either NH_2OH or O_2 easily, serving as electron acceptors or donors [31,32].

4. Conclusions

Selective surface modification of AC by mild $KMnO_4$ oxidation yielded more quinones but less carboxylic groups, and thus enhanced the production of H_2O_2 by NH_2OH oxidation with a H_2O_2 yield of 78% (0.66 wt.%). Comparative tests using homogeneous organic compounds as catalysts confirmed that the quinonoid

species might be the active species which involved in the reaction network through a redox mechanism. The quinonoid species initially interacted with NH_2OH to form H_2O_2 and the reduced species like semiquinones or hydroquinones reacted with molecular oxygen, realizing the redox cycle.

References

[1] J.M. Campos-Martin, G. Blanco-Brieva, J.L.G. Fierro, Angew. Chem. Int. Ed. 45 (2006) 6962–6984.
[2] M.G. Clerici, P. Ingallina, Catal. Today 41 (1998) 351–364.
[3] C. Perego, A. Carati, P. Ingallina, M.A. Mantegazza, G. Bellussi, Appl. Catal. A 221 (2001) 63–72.
[4] J.H. Lunsford, J. Catal. 216 (2003) 455–460.
[5] C. Samanta, Appl. Catal. A 350 (2008) 133–149.
[6] S. Niwa, M. Eswaramoorthy, N. Jalajakumari, R. Anju, I. Naotsugu, S. Hiroshi, N. Takemi, M. Fujio, Science 295 (2002) 105–107.
[7] M.N. Hughes, H.G. Nicklin, J. Chem. Soc. A 1 (1971) 164–168.
[8] T.S. Sheriff, J. Chem. Soc. Dalton Trans. 6 (1992) 1051–1058.
[9] T.S. Sheriff, P. Carr, B. Piggott, Inorg. Chim. Acta 348 (2003) 115–122.
[10] T.S. Sheriff, P. Carr, S.J. Coles, M.B. Hursthouse, J. Lesin, M.E. Light, Inorg. Chim. Acta 357 (2004) 2494–2502.
[11] V.R. Choudhary, P. Jana, S.K. Bhargava, Catal. Commun. 8 (2007) 811–816.
[12] V.R. Choudhary, P. Jana, Catal. Commun. 8 (2007) 1578–1582.
[13] V.R. Choudhary, P. Jana, Appl. Catal. A 335 (2008) 95–102.
[14] W. Song, J. Li, J. Liu, W. Shen, Catal. Commun. 9 (2008) 831–836.
[15] H. Teng, Y.T. Tu, Y.C. Lai, C.C. Lin, Carbon 39 (2001) 575–582.
[16] J. Zhang, H. Zou, Q. Qing, Y. Yang, Q. Li, Z. Liu, X. Guo, Z. Du, J. Phys. Chem. B 107 (2003) 3712–3718.
[17] J.Y. Howe, M.D. Dadmun, P.F. Britt, Carbon 45 (2007) 1072–1080.
[18] H.P. Boehm, Carbon 32 (1994) 759–769.
[19] F.J. López-Garzón, M. Domingo-García, M. Pérez-Mendoza, P.M. Alvarez, V. Gómez-Serrano, Langmuir 19 (2003) 2838–2844.
[20] J.L. Figueiredo, M.F.R. Pereira, M.M.A. Freitas, J.J.M. Órfão, Carbon 37 (1999) 1379–1389.
[21] P.A. Clapp, D.F. Evans, T.S. Sheriff, Anal. Chim. Acta 218 (1989) 331–334.
[22] M. Yang, Huagong Xuebao (Chin. Ed.) 16 (1999) 233–235.
[23] D. Prahas, Y. Kartika, N. Indraswati, S. Ismadji, Chem. Eng. J. 140 (2008) 32–42.
[24] A. Macías-García, M.A. Díaz-Díez, E.M. Cuerda-Correa, M. Olivares-Marín, J. Gañan-Gómez, Appl. Surf. Sci. 252 (2006) 5972–5975.
[25] G. de la Puente, J.J. Pis, J.A. Menéndez, P. Grange, J. Anal. Appl. Pyrol. 43 (1997) 125–138.
[26] A.P. Terzyk, Colloids Surf. A 177 (2001) 23–45.
[27] D.V. Brazhnyk, Y.P. Zaitsev, I.V. Bacherikova, V.A. Zazhigalov, J. Stoch, A. Kowal, Appl. Catal. B 70 (2007) 557–566.
[28] A. Swiatkowski, M. Pakula, S. Biniak, M. Walczyk, Carbon 42 (2004) 3057–3069.
[29] H.P. Boehm, Carbon 40 (2002) 145–149.
[30] U. Zielke, K.J. Hüttinger, W.P. Hoffman, Carbon 34 (1996) 983–998.
[31] P. Serp, J.L. Figueiredo, Carbon Materials for Catalysis, Wiley, New Jersey, 2009, pp. 177–208.
[32] F.P. Van Der Zee, I.A.E. Bisschops, G. Lettinga, Environ. Sci. Technol. 37 (2003) 402–408.